

Electronic Supplementary Information

Activated Carbon Becomes Active for Oxygen Reduction and Hydrogen Evolution Reactions

Xuecheng Yan,^a Yi Jia,^a Taiwo Odedairo,^b Xiaojun Zhao,^a Zhao Jin,^a Zhonghua Zhu^b and Xiangdong Yao^{*ac}

^aQueensland Micro- and Nanotechnology Centre, Griffith University,
Nathan Campus, QLD 4111, Australia

*E-mail: x.yao@griffith.edu.au

^bSchool of Chemical Engineering, The University of Queensland,
St Lucia, Brisbane, Queensland 4072, Australia

^cSchool of Natural Sciences, Griffith University,
Nathan Campus, QLD 4111, Australia

Experimental Section

(1) Materials Synthesis

In a typical preparation, a kind of activated carbon (Ningxia Huahui Activated Carbon Company Limited, China) was selected for the study. To introduce nitrogen into the activated carbon sample, it was treated under pure NH₃ atmosphere at 500 °C for 3 h with the flow rate of 30 mL/min (N-AC), the final sample was obtained *via* calcining the N-doped carbon at 1050 °C for 2 h under nitrogen conditions (denoted as D-AC because it is a kind of defective activated carbon).

(2) Characterizations

Chemical compositions of the prepared samples were acquired using a Kratos Axis ULTRA X-ray photoelectron spectrometer incorporating a 165 mm hemispherical electron energy analyzer. The incident radiation is Monochromatic Al K α X-rays (1486.6 eV) at 150 W (15 kV, 10 mA). The morphologies and structures of the materials were examined by using transmission electron microscopy (TEM) (Hitachi 800) and high-resolution TEM (HRTEM) (JEOL JEM-2100). Raman spectra were recorded on a Renishaw InVia spectrometer using the 514 nm laser excitation. The nitrogen adsorption and desorption isotherms were measured at the temperature of liquid nitrogen (77 K) using a TriStar II 3020 automated surface area and pore size analyzer. Specific surface area was calculated from the adsorption data according to the Brunauer-Emmett-Teller (BET) method. The pore-size distribution was obtained by using the density functional theory (DFT) model. Prior to the measurement, samples were degassed at 150 °C overnight.

(3) Electrochemical Measurements

The typical three-electrode system was utilized to evaluate the electrochemical properties of the prepared catalysts. Specifically, glassy carbon (GC) is the working electrode, a Pt wire is the counter electrode and the Ag/AgCl (in saturated KCl solution) is the reference electrode. All potentials were referred to the reversible hydrogen electrode by adding a value of $(0.197 + 0.059 \cdot \text{pH})$ V and all the tests were

performed without iR compensation. Cyclic voltammetry (CV), linear sweep voltammetry (LSV) and rotating ring-disk electrode (RRDE) measurements were conducted on the CHI 760E workstation (CH Instruments, Inc.) with a RRDE-3A rotator (ALS Co., Ltd).

Sample Preparation: 1 mg of the catalyst was dispersed into the 1 mL mixed solution of distilled water (680 μL), ethanol (300 μL) and Nafion® 117 Solution (5%, 20 μL). Then, different volumes of the mixture were dropped onto the polished glassy carbon electrodes for ORR and HER tests after sonicating it for at least 60 min to form a homogeneous ink. The loaded electrode was placed in the 60 °C oven for 10 min to dry and then take it out to cool down before all the tests.

ORR Measurement

Catalyst Loading. 10 μL of the mixture was dropped onto the polished glassy carbon electrode (4 mm in diameter, catalyst loading: 0.08 $\text{mg}\cdot\text{cm}^{-2}$).

Cyclic voltammetry (CV). Prior to the test, the electrolyte (0.1 mol/L KOH solution) was bubbled with O_2 for at least 30 min to make sure it saturated with O_2 , and keep a constant oxygen flow during the measurement. The data was recorded at the scan rate of 100 mV/s when the system became stable.

Linear sweep voltammetry (LSV) measurement. The rotating speed of the working electrode increased from 400 rpm to 2500 rpm at the scan rate of 10 mV/s in O_2 -saturated 0.1 M KOH solution.

Koutecky-Levich (K-L) plots. The working electrode was scanned cathodically at the rate of 10 mV/s with the rotation speed from 400 to 2500 rpm. Koutecky-Levich (K-L) plots (J^1 vs $\omega^{-1/2}$) were analyzed at different potentials.

Koutecky-Levich equation:^{1,2}

$$\frac{1}{J} = \frac{1}{J_L} + \frac{1}{J_K} = \frac{1}{B\omega^{1/2}} + \frac{1}{J_K}$$

$$B = 0.2nFC_0D_0^{2/3}\nu^{-1/6}; J_K = nFkC_0$$

where J is the measured current density, J_k and J_L are the kinetic and limiting current densities, ω is the angular velocity, n is transferred electron number, F (96485 C/mol) is the

Faraday constant, D_0 is the diffusion coefficient of O_2 in 0.1 M KOH ($1.9 \times 10^{-5} \text{ cm}^2/\text{s}$), C_0 is the bulk concentration of O_2 ($1.2 \times 10^{-6} \text{ mol}/\text{cm}^3$), ν is the kinetic viscosity of the electrolyte ($0.01 \text{ cm}^2/\text{s}$) and k is the electron-transfer rate constant. The constant 0.2 is adopted when the rotation speed is expressed in rpm.

Rotating ring-disk electrode (RRDE) measurement. The rotating speed of the working electrode was fixed at 1600 rpm with the scan rate of 10 mV/s in O_2 -saturated 0.1 M KOH solution for the RRDE test. The electron transfer number (n) and the percentage of HO_2^- and were calculated *via* the following equations.^{3,4}

$$n = 4I_d / (I_d + I_r / N) \quad (S1)$$

$$\% HO_2^- = 200(I_r / N) / (I_d + I_r / N) \quad (S2)$$

Where I_d stands for the disk current, I_r represents the ring current, and N is the current collection efficiency of the Pt ring, which was identified to be 0.43 in 2 mmol/L $K_3Fe[CN]_6$ and 0.1 mol/L KCl solution.

HER Measurement

Catalyst Loading. 5 μL of the mixture was dropped onto the polished glassy carbon electrode (3 mm in diameter, catalyst loading: $0.07 \text{ mg}\cdot\text{cm}^{-2}$).

Linear sweep voltammetry (LSV) measurement. The rotating speed of the working electrode was maintained at 1600 rpm at the scan rate of 10 mV/s in 0.5 M H_2SO_4 solution.

Chronoamperometric measurement ($\eta = 400 \text{ mV}$) was performed to evaluate the long-term stability of sample D-AC.

Table S1. XPS results analysis for the prepared samples.

Sample Name	C (Atom%)	N (Atom%)	O (Atom%)
H-AC	94.10	----	5.90
N-AC	93.91	3.73	2.36
D-AC	99.23	----	0.77

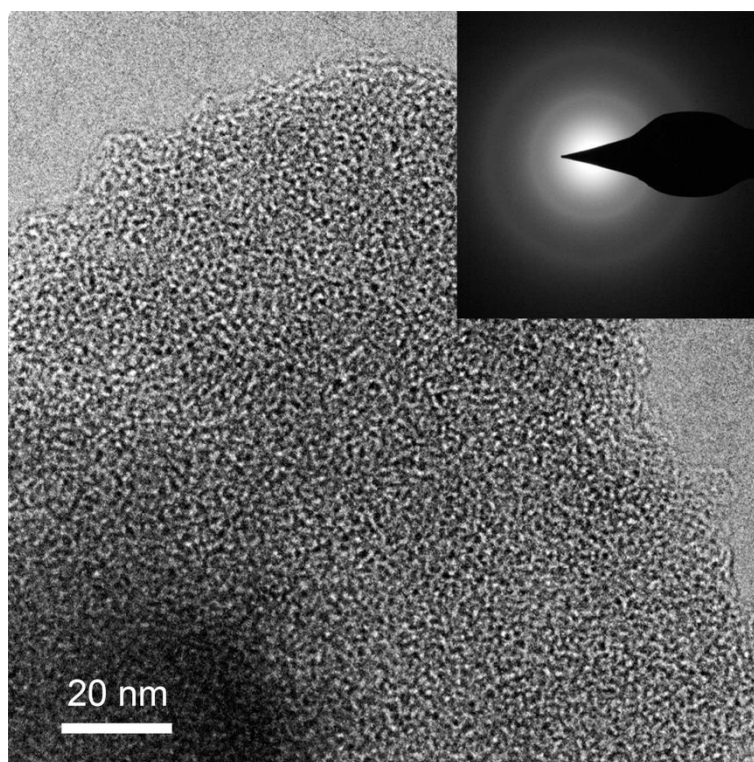


Figure S1. TEM image showing the microstructure of the D-AC and the corresponding SAED pattern.

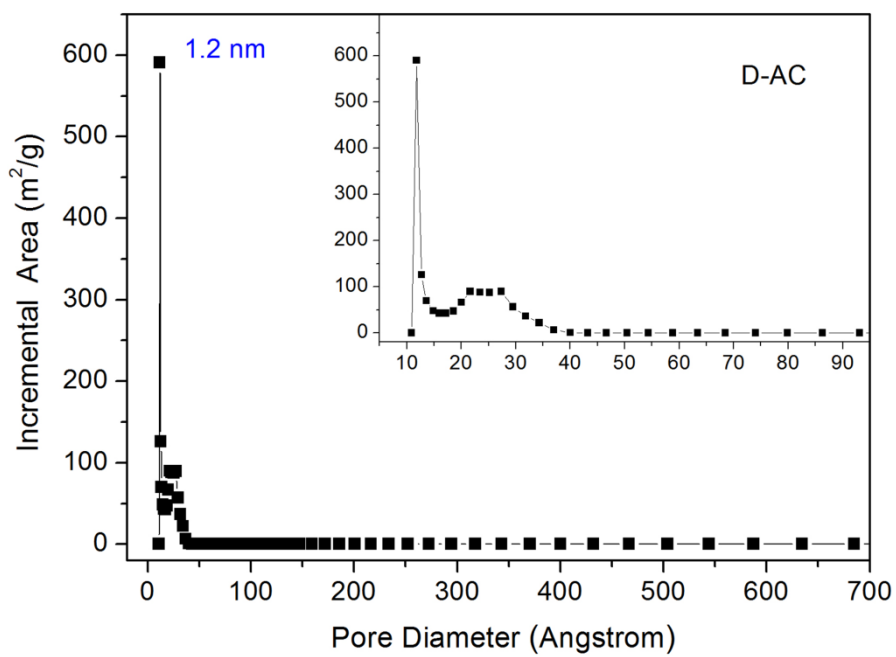


Figure S2. Pore size distribution of the prepared sample D-AC.

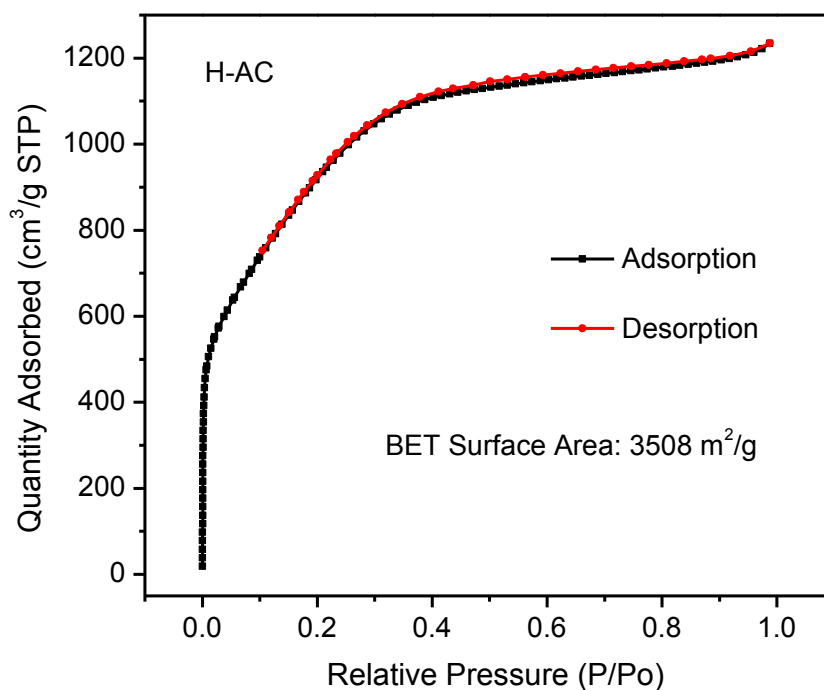


Figure S3. Nitrogen adsorption-desorption isotherm of the prepared sample H-AC.

Table S2. Textural Parameters of the Samples

Sample Name	S_{BET}^a (m^2/g)	Pore Size ^b (nm)	V_{total}^c (cm^3/g)	V_{micro}^d (cm^3/g)	V_{meso}^e (cm^3/g)	$V_{\text{micro}}/V_{\text{total}}$ (%)
H-AC	3508	1.2	1.909	1.381	0.528	72.3
N-AC	3280	1.2	1.766	1.302	0.464	73.7
D-AC	2986	1.2	1.555	1.072	0.483	68.9

^a S_{BET} is specific surface area that calculated via the Brunauer-Emmett-Teller (BET) method.

^b Pore size distribution is identified by density functional theory (DFT) approach. ^c The total pore volume is calculated at the highest relative pressure in the adsorption process. ^d The micropore volume is determined by Dubinin-Astakhov (DA) analysis. ^e The mesopore volume is received by subtracting the micropore volume from the total pore volume.

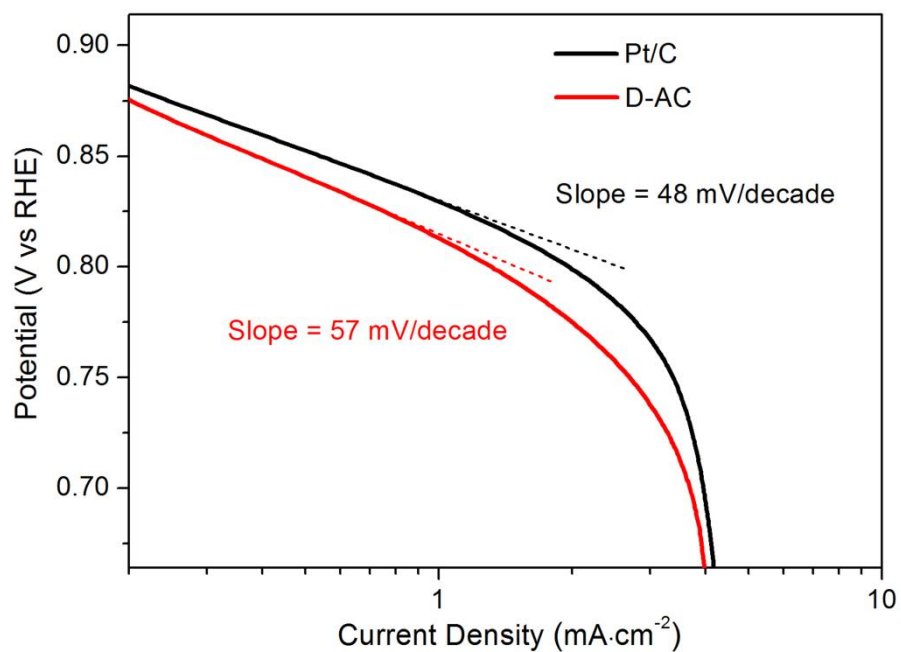


Figure S4. Tafel plots derived from the corresponding 1600 rpm LSV curves of the D-AC and Pt/C.

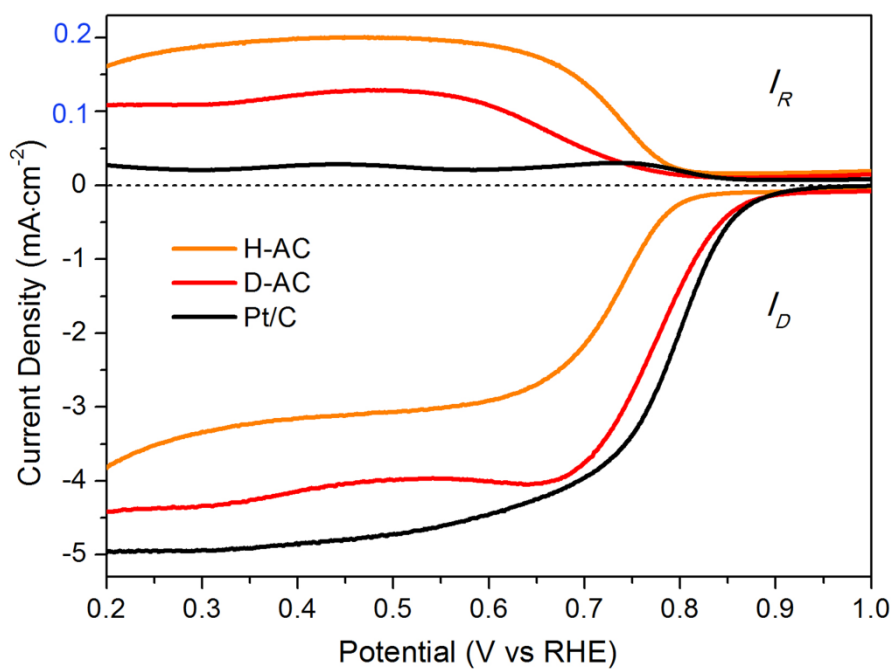


Figure S5. Rotating ring-disk electrode voltammogram of the H-AC, D-AC and Pt/C in O₂-saturated 0.1 M KOH solution at 1600 rpm.

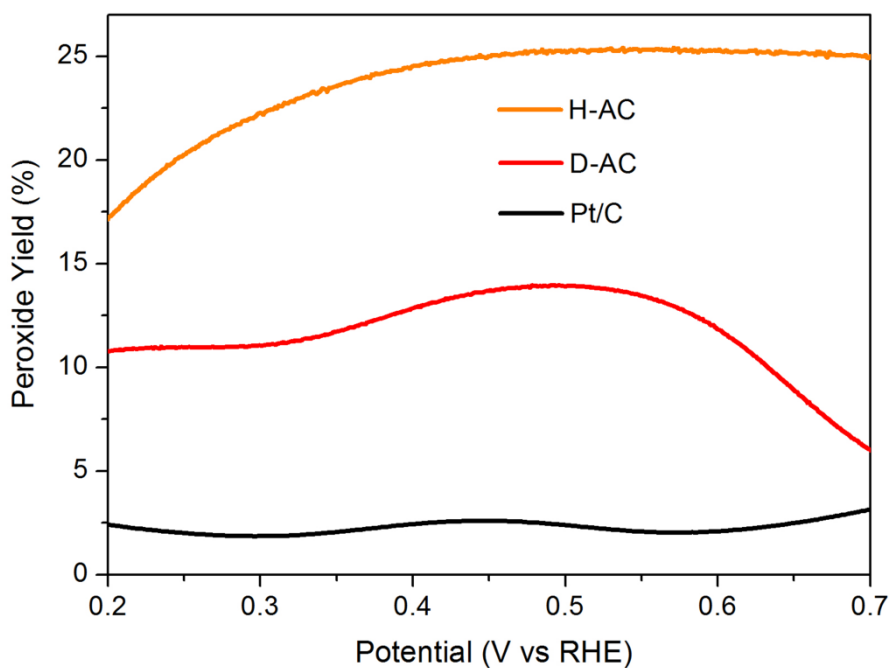


Figure S6. Percentages of peroxide with respect to the total oxygen reduction products of the H-AC, D-AC and Pt/C in O₂-saturated 0.1 M KOH solution at 1600 rpm.

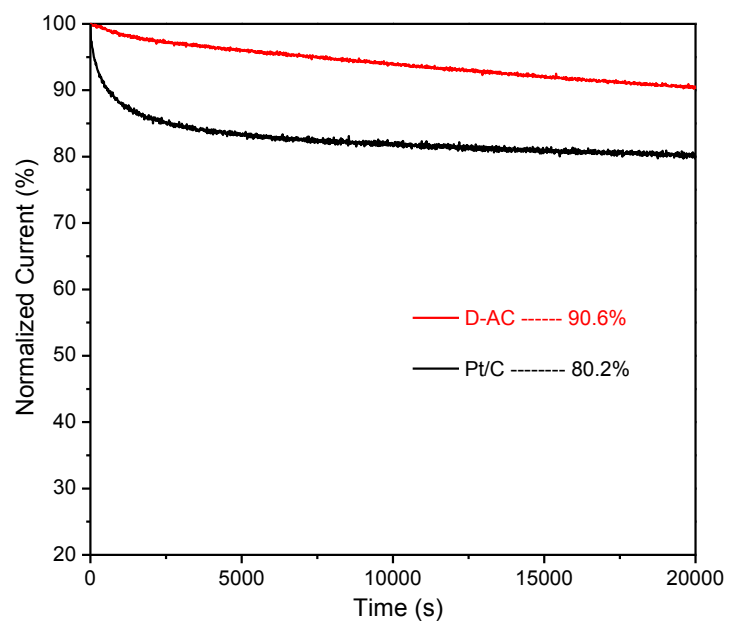


Figure S7. Amperometric *i-t* curves of the D-AC and Pt/C that measured in O₂-saturated 0.1 M KOH solution with the rotating speed of 1000 rpm.

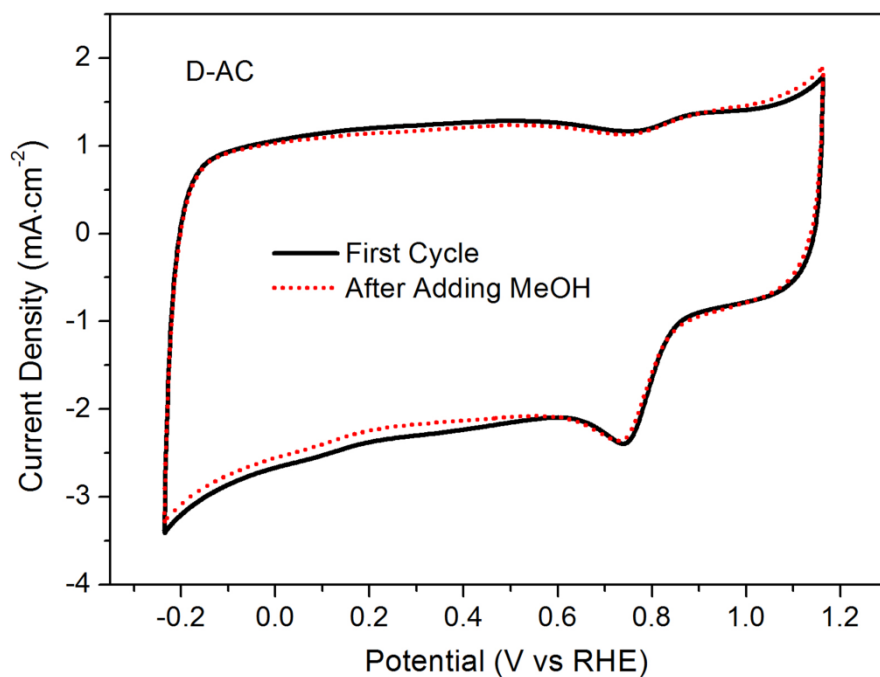


Figure S8. Methanol tolerance test with 5% methanol (in volume) in O₂-saturated 0.1 M KOH solution for the D-AC.

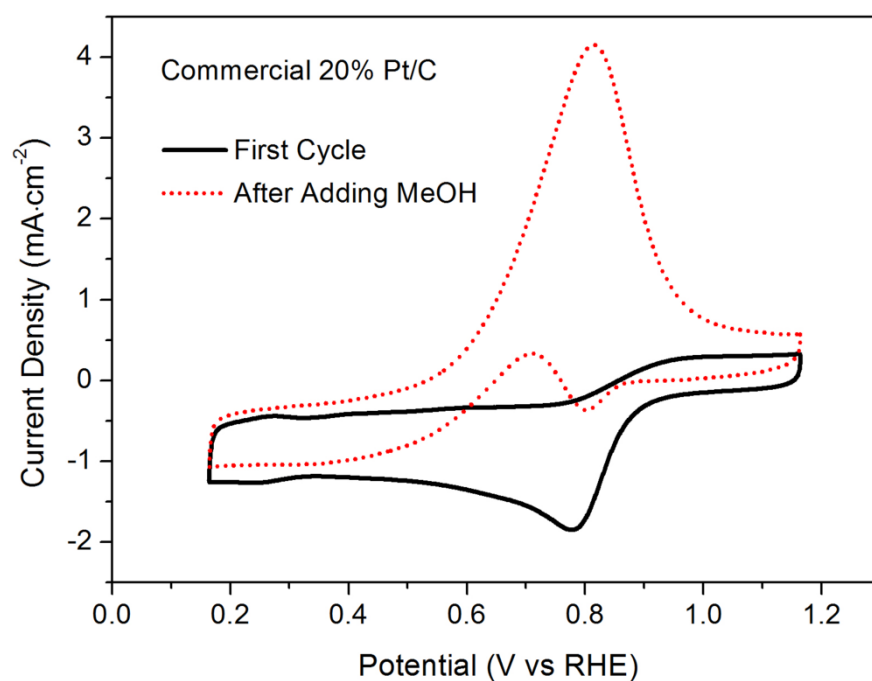


Figure S9. Methanol tolerance test with 5% methanol (in volume) in O₂-saturated 0.1 M KOH solution for the Pt/C.

Table S3. Summary of the half-wave potential ($E_{1/2}$) for the reported metal-free ORR electrocatalysts.

Catalyst	Half-wave potential (mV vs. RHE)	Reference
N-doped Ordered Mesoporous Graphitic Arrays	~ 0.69	5
P-doped Ordered Mesoporous Carbon	~ 0.72	6
P-doped Ordered Mesoporous Carbon	~ 0.75	7
Graphene Quantum Dots Supported by Graphene Nanoribbons	~ 0.80	8
N-doped Carbon Nanosheets	~ 0.83	9
H-AC	0.714	This Work
N-AC	0.707	
D-AC	0.771	

Note: The ORR measurements were conducted in O₂-saturated 0.1 M KOH solution.

Table S4. Onset overpotentials, Tafel slopes and operating potential at -10 mA/cm^2 of metal-free HER catalysts reported in the literature.

Catalyst	Onset Potential (mV vs. RHE)	Tafel Slope (mV/decade)	η (mV) at $j = -10 \text{ mA/cm}^2$	Reference
N-graphene	331	116	490	10
P-graphene	374	133	553	
N,P-graphene	289	91	422	
$\text{C}_3\text{N}_4@\text{NG}$	~ 160	51.5	240	11
N-graphene	316	506	506	12
Activated carbon nanotubes	100	71	~ 225	13
g- C_3N_4 nanoribbon-G	80	54	207	14
NS co-doped graphene	130	81	276	15
H-AC	257	102	390	This Work
N-AC	216	137	346	
D-AC	198	66	334	

Note: The HER tests were carried out in 0.5 M H_2SO_4 solution.

References

1. Y. Liang, H. Wang, J. Zhou, Y. Li, J. Wang, T. Regier and H. Dai, *J. Am. Chem. Soc.*, 2012, **134**, 3517-3523.
2. S. Wang, D. Yu, L. Dai, D. W. Chang and J.-B. Baek, *ACS Nano*, 2011, **5**, 6202-6209.
3. U. A. Paulus, T. J. Schmidt, H. A. Gasteiger and R. J. Behm, *J. Electroanal. Chem.*, 2001, **495**, 134-145.
4. Y. Liang, Y. Li, H. Wang, J. Zhou, J. Wang, T. Regier and H. Dai, *Nat. Mater.*, 2011, **10**, 780-786.
5. R. Liu, D. Wu, X. Feng and K. Müllen, *Angew. Chem. Int. Ed.*, 2010, **49**, 2565-2569.
6. D.-S. Yang, D. Bhattacharjya, S. Inamdar, J. Park and J.-S. Yu, *J. Am. Chem. Soc.*, 2012, **134**, 16127-16130.
7. S. Lee, M. Choun, Y. Ye, J. Lee, Y. Mun, E. Kang, J. Hwang, Y. H. Lee, C. H. Shin, S. H. Moon, S. K. Kim and E. Lee, *Angew. Chem. Int. Ed.*, 2015, **54**, 9230-9234.
8. H. Jin, H. Huang, Y. He, X. Feng, S. Wang, L. Dai and J. Wang, *J. Am. Chem. Soc.*, 2015, **137**, 7588-7591.
9. W. Wei, H. W. Liang, K. Parvez, X. D. Zhuang, X. L. Feng and K. Mullen, *Angew. Chem. Int. Ed.*, 2014, **53**, 1570-1574.
10. Y. Zheng, Y. Jiao, L. H. Li, T. Xing, Y. Chen, M. Jaroniec and S. Z. Qiao, *ACS Nano*, 2014, **8**, 5290-5296.
11. Y. Zheng, Y. Jiao, Y. Zhu, L. H. Li, Y. Han, Y. Chen, A. Du, M. Jaroniec and S. Z. Qiao, *Nat. Commun.*, 2014, **5**, 3783.
12. L. Wei, H. E. Karahan, K. Goh, W. Jiang, D. Yu, O. Birer, R. Jiang and Y. Chen, *J. Mater. Chem. A*, 2015, **3**, 7210-7214.
13. W. Cui, Q. Liu, N. Cheng, A. M. Asiri and X. Sun, *Chem. Commun.*, 2014, **50**, 9340-9342.
14. Y. Zhao, F. Zhao, X. Wang, C. Xu, Z. Zhang, G. Shi and L. Qu, *Angew. Chem. Int. Ed.*, 2014, **53**, 13934-13939.
15. Y. Ito, W. Cong, T. Fujita, Z. Tang and M. Chen, *Angew. Chem. Int. Ed.*, 2015, **54**, 2131-2136.